Published in final edited form as:
Circ Res. 2008 October 24; 103(9): 1018–1026. doi:10.1161/CIRCRESAHA.108.178459.

Overexpression of VEGF-B in mouse heart alters cardiac lipid metabolism and induces myocardial hypertrophy

Terhi Karpanen[*,1,8], **Maija Bry**[1,*], **Hanna M. Ollila**[1], **Tuulikki Seppänen-Laakso**[3], **Erkki Liimatta**[4], **Hanna Leskinen**[5], **Riikka Kivelä**[1], **Teemu Helkamaa**[2], **Mari Merentie**[6], **Michael Jeltsch**[1], **Karri Paavonen**[1], **Leif C. Andersson**[7], **Eero Mervaala**[2], **Ilmo E. Hassinen**[4], **Seppo Ylä-Herttuala**[6], **Matej Orešič**[3], and **Kari Alitalo**[1]

[1]Molecular/Cancer Biology Laboratory and Ludwig Institute for Cancer Research, Biomedicum Helsinki and Haartman Institute, University of Helsinki and Helsinki University Central Hospital, Helsinki, Finland [2]Institute of Biomedicine, Department of Pharmacology, University of Helsinki and Helsinki University Central Hospital, Helsinki, Finland [3]VTT Technical Research Centre of Finland, Espoo, Finland [4]Department of Medical Biochemistry and Molecular Biology, University of Oulu, Oulu, Finland [5]Department of Pharmacology and Toxicology, University of Oulu, Oulu, Finland [6]A.I. Virtanen Institute, Department of Biotechnology and Molecular Medicine, University of Kuopio, Kuopio, Finland [7]Department of Pathology, Haartman Institute, University of Helsinki, Helsinki, Finland

Abstract

Vascular Endothelial Growth Factor-B (VEGF-B) is poorly angiogenic but prominently expressed in metabolically highly active tissues, including the heart. We produced mice expressing a cardiac-specific VEGF-B transgene via the alpha myosin heavy chain promoter. Surprisingly, the hearts of the VEGF-B transgenic mice showed concentric cardiac hypertrophy without significant changes in heart function. The cardiac hypertrophy was due to an increased size of the cardiomyocytes. Blood capillary size was increased, while the number of blood vessels per cell nucleus remained unchanged. Despite the cardiac hypertrophy, the transgenic mice had lower heart rate and blood pressure than their littermates, and they responded similarly to angiotensin II-induced hypertension, confirming that the hypertrophy does not compromise heart function. Interestingly, the isolated transgenic hearts had less cardiomyocyte damage after ischemia. Significantly increased ceramide and decreased triglyceride levels were found in the transgenic hearts. This was associated with structural changes and eventual lysis of mitochondria, resulting in accumulation of intracellular vacuoles in cardiomyocytes and increased death of the transgenic mice, apparently due to mitochondrial lipotoxicity in the heart. These results suggest that VEGF-B regulates lipid metabolism, an unexpected function for an angiogenic growth factor.

Keywords

VEGF-B; cardiac hypertrophy; cardiac metabolism; fatty acids; mitochondria

Address correspondence to Kari Alitalo, MD, PhD, Molecular/Cancer Biology Laboratory, Biomedicum Helsinki, P.O.B. 63, FI-00014 Helsinki, Finland; Tel: +358919125511, Fax: +358919125510, kari.alitalo@helsinki.fi.
[8]Present address: Hubrecht Institute, Utrecht, Netherlands
[*]These authors contributed equally to this work

Disclosures
None

Introduction

Members of the Vascular Endothelial Growth Factor (VEGF) family, currently comprising five mammalian proteins, are major regulators of blood and lymphatic vessel development and growth. VEGF is essential for vasculogenesis and angiogenesis, whereas VEGF-C is necessary for lymphangiogenesis. Although not required for embryonic development, placenta growth factor (PlGF) and VEGF-D are likely to play more subtle roles in the control of angiogenesis and lymphangiogenesis, or function under pathological conditions[1,2].

VEGF-B exists as two isoforms generated by alternative splicing. VEGF-B_{167} has a heparin-binding carboxy-terminus, whereas VEGF-B_{186} contains a hydrophobic carboxy-terminus, is O-glycosylated and proteolytically processed[3]. Both isoforms bind to VEGF receptor-1 (VEGFR-1) and neuropilin-1 (NRP-1), but not to the major mitogenic endothelial cell receptors VEGFR-2 or VEGFR-3[4,5].

VEGF-B has a wide tissue distribution, being most abundant in the myocardium, skeletal and vascular smooth muscle, as well as in brown adipose tissue[6]. Mice lacking VEGF-B are viable and fertile and display only a mild phenotype in the heart. This is manifested as an atrial conduction abnormality characterized by a prolonged PQ interval in one strain (C57Bl background)[7], or as a smaller heart size with impaired recovery after myocardial ischemia in another (129/SvJ or 129/SvJxC57Bl/6J background)[8]. Furthermore, VEGF-B has also been implicated in pathological vascular changes in inflammatory arthritis[9] and in protecting the brain from ischemic injury[10]. However, the ability of VEGF-B to stimulate angiogenesis directly is poor in many tissues. VEGF-B did not stimulate vessel growth when delivered into muscle or periadventitial tissue via adenoviral vectors[11,12]. On the contrary, VEGF-B overexpressed in endothelial cells of transgenic mice was able to potentiate, rather than initiate, angiogenesis[13]. And unlike VEGF, VEGF-B did not increase vascular permeability[8,13].

Here we have studied the effects of VEGF-B in the skin and heart, by overexpression via the keratin-14 (K14) and alpha myosin heavy chain (αMyHC) promoters, respectively. VEGF-B promoted very little angiogenesis. However, mice overexpressing VEGF-B in the heart gradually developed cardiac hypertrophy with increased cardiomyocyte size and, surprisingly, had lower blood pressure, lower heart rate and larger blood vessels in the myocardium than their wildtype littermates. The hypertrophy was associated with changes in mitochondrial morphology and eventual lysis of mitochondria. We found marked changes in the lipidomic profiles of the transgenic hearts, including increased amounts of ceramides. These results suggest that VEGF-B is capable of altering cardiac lipid metabolism, with overexpression ultimately leading to cardiomyopathy.

Materials and Methods

A detailed description is provided as supplemental material.

Generation of transgenic mice

To generate K14-VEGF-B transgenic mice, DNA from the human VEGF-B gene was cloned into the K14 expression vector (provided by Dr. Elaine Fuchs). To generate the heart-specific transgene, cDNA encoding human VEGF-B_{167}[14] was ligated into the αMyHC promoter expression vector (a gift from Dr. Jeffrey Robbins). Expression cassettes were injected into fertilized mouse oocytes of FVB background. Mice were PCR-genotyped using tail DNA. All mouse experiments were approved by the Provincial State Office of Southern Finland and carried out in accordance with institutional guidelines.

Immunohistochemistry

Sections of paraformaldehyde-fixed, paraffin-embedded mouse hearts were stained with rat antibodies against mouse Pecam-1 (BD Pharmingen) using biotinylated anti-rat IgG (Vector Laboratories) and TSA-kit (NEN Life Sciences) for detection. The number and size of Pecam-1 stained vessels were quantified using ImageJ program (NIH). Results are presented as average ±SD.

Acetone-fixed cryosections were stained with antibodies against collagen IV (CosmoBio), laminin-1 (a gift from Päivi Liesi), VEGFR-1 (a gift from Dr. Bronek Pytowski, ImClone Systems), neuropilin-1 or VEGF-B (R&D Systems). AlexaFluor488-conjugated anti-rabbit or AlexaFluor594-conjugated anti-goat (Molecular Probes) antibodies were used for detection. Cardiomyocyte sizes were quantified from laminin-1-stained photomicrographs using Axiovision program (Zeiss).

Echocardiography

Transthoracic echocardiography was performed using Acuson Ultrasound System (Sequoia™512) and a 15-MHz linear transducer. Mice were anesthetized with fentanyl citrate, fluanisone and midazolam, and normal body temperature was maintained.

Telemetric analysis

Heart rate and mean arterial pressure were recorded from left carotid artery using telemetric implants as previously described[15], except xylazine was used for anaesthesia. Data collection was started on the fifth day when the normal circadian rhythm of the mice had returned. Data were gathered day and night for two weeks, every 5 min for 10 s.

Measurements of mitochondrial redox state and tolerance of short-term ischemia in isolated, perfused hearts

Aorta was cannulated immediately after cervical dislocation and perfusion commenced. The heart was enclosed in a thermostatic, light-tight chamber connected to a spectrophotometer-fluorometer. Left ventricular pressure was monitored using a saline-filled cannula connected to a Statham P231D pressure transducer and SP1400 pressure monitor. Parameters were calculated with custom-designed software. Venous effluent from the heart was collected in 1 min aliquots and lactate dehydrogenase washout measured. The values are presented as mean ±SE.

Angiotensin II-induced pressure overload

Angiotensin II was administered via subcutaneous Alzet-minipumps (Scanbur AB) for 1 week (0.1mg/kg/h). Echocardiography was performed using VEVO 779 Ultrasound System (VisualSonics).

Electron microscopy

Left ventricular samples were fixed with glutaraldehyde, postosmicated and embedded in epon. Regions of interest were examined with JEOL 1400 EX Transmission Electron Microscope.

Lipidomic analysis of heart tissue

Lipid extracts of heart tissue, mixed with a labeled lipid standard mixture, were analyzed on a Waters Q-Tof Premier mass spectrometer combined with Acquity Ultra Performance liquid chromatography. Results are presented as mean±SEM.

Results

VEGF-B is minimally angiogenic in the skin

We generated transgenic mice overexpressing VEGF-B in the epidermis under the K14-promoter (Supplemental Figure 1A–B). Dermal vessel density and branching were only slightly increased (~20%; Supplemental Figure 1C), thus VEGF-B only minimally promoted angiogenesis in the skin.

VEGF-B encoded by a heart-specific transgene is associated with pericellular matrix

As the heart is one of the major sites of VEGF-B expression and the primary organ affected upon deletion of the VEGF-B gene, we studied the effects of VEGF-B in this tissue. For this, we overexpressed the heparin-binding VEGF-B isoform, VEGF-B_{167}, under the alpha myosin heavy chain, αMyHC, promoter (Figure 1A). The VEGF-B_{167} transgene was expressed at 6 and 8-fold compared to the endogenous VEGF-B gene in the myocardium of the two transgenic mouse lines studied, as analyzed by Northern and Western blotting (Supplemental Figure 1D and data not shown), and by immunohistochemistry (Figure 1B). Much of the extracellular VEGF-B_{167} protein colocalized with the pericellular matrix component collagen IV (Figure 1B). Intracellular staining was also observed in denatured samples (Figure 1B, lower row middle). VEGFR-1 and NRP-1 distribution partially overlapped with that of collagen IV and laminin (Figure 1B–C and data not shown), suggesting that extracellular VEGF-B was bound to heparan sulphates in the basal laminae of myocardial blood vessels and cardiomyocytes.

The hearts of the αMyHC-VEGF-B_{167} mice display cardiac hypertrophy, but no significant change in systolic function

The hearts of the transgenic mice appeared bigger and more muscular than the hearts of their wildtype littermates (Figure 2A). In cross sections the walls of the left ventricle were thicker and the cardiomyocytes larger (Figure 2B–C). Hypertrophy of the cardiomyocytes was confirmed by cell area quantification from sections stained for laminin-1 (Figure 2C–D). The heart to body weight ratio was significantly higher in the transgenic mice when compared to their littermates (5.93±1.36mg/g for TG males, average±SD, n=16, as compared to 4.95 ±0.78mg/g for WT males, n=16, p<0.02, Figure 2E). A higher heart weight to body weight ratio was also observed in female transgenic mice (data not shown).

Echocardiography confirmed the left ventricular hypertrophy in the αMyHC-VEGF-B_{167} mice as measured by the thickness of the left ventricular posterior wall (Figure 2F) and interventricular septum (Figure 2G) in diastole and by the functional left ventricular mass (Figure 2H). No change was observed in diastolic left ventricular diameter (Table 1). The cardiac hypertrophy was more severe in male mice and increased with age (Figure 2F–H). However, there was no change in systolic function as measured by ejection fraction and fractional shortening (Table 1).

Telemetric measurement revealed that the transgenic heart rate was significantly lower than the heart rate of wildtype littermates (511±52 beats/minute for TG, n=3, vs 635±20 beats/minute for WT mice, n=5, p<0.001; Figure 3A). Both systolic and diastolic blood pressures were also lower in the transgenic mice (128±3.6 mmHg vs 143±5.1 mmHg in systole and 94 ±3.7 mmHg vs 109±5.5 mmHg in diastole, for TG, n=3, and WT, n=5, mice, respectively, p<0.001; Figure 3B and Supplemental Figure 2). However, αMyHC-VEGF-B_{167} mice under anesthesia had ventricular extrasystoles and were more prone to arrhythmias (20/28 of TG vs 5/29 of WT mice at 12 months of age). We also observed an increase in the death rate of the transgenic mice (Figure 3C).

The hearts of the αMyHC-VEGF-B_{167} mice have larger blood vessels

Immunohistochemical staining for Pecam-1 revealed a lower blood vessel density in the hearts of αMyHC-VEGF-B_{167} mice than in wildtype littermates (236±33 vs 297±38 vessels/microscopic field, n=13, p<0.001; Figure 4A–C). However, when calculated per number of cardiomyocyte nuclei in the analyzed area, the number of vessels in transgenic hearts was comparable to that of wildtype hearts (1.68±0.19, n=7, vs 1.95±0.24, n=5, p>0.05, Figure 4D). The blood vessels in the myocardium of the αMyHC-VEGF-B_{167} mice were larger than those of their littermates (average vessel area 1223±244 vs 944±130 pixels, p<0.002, Figure 4E). This was associated with an increase in the number of endothelial cells per vessel cross-section (0.64±0.11, n=6, vs 0.51±0.09, n=4, p<0.004). Thus, the total area covered by blood vessels in the myocardium of the transgenic mice was similar to that of controls (277236±44831 vs 274278±37929 pixels/microscopic field, p>0.5, Figure 4F). This indicates that while VEGF-B_{167} overexpression did not affect the vessel number per cardiomyocyte, the vessel area per cardiomyocyte was increased.

Mitochondrial redox state

Central for energy metabolism and heart function is fatty acid oxidation coupled to ATP production in mitochondria. The myocardial content of cytochrome c oxidase (cytochrome aa_3), a marker of the mitochondrial respiratory chain, was similar in transgenic and control hearts. The steady state oxidation-reduction level of cytochrome aa_3 tended to be slightly more reduced in transgenic hearts than in controls (Figure 5A–B), which was also the case for the fluorescent flavoproteins. These mainly reflect the activity of mitochondrial lipoamide dehydrogenase, which is in equilibrium with the NADH/NAD pool[16] and can therefore be used as a redox indicator for NADH/NAD in the mitochondrial matrix. When the cytochrome aa_3 reduction percentage was plotted against mechanical work output during electrical pacing to varying heart rates, the plots were linear without a significant difference between the slopes of transgenic and control hearts. Cytochrome aa_3 reduction at the intercept (representing zero work output) was similar for both transgenic and control hearts, indicating no difference in the mitochondrial coupling efficiency (data not shown).

Ischemia and pressure overload tolerance

Lactate dehydrogenase washout from the transgenic hearts after a 20 min period of ischemia was significantly less than from wildtype controls (Figure 5C), suggesting less cellular damage upon ischemia-reperfusion. Despite this indication of myocardial protection, the relative work output (pressure development × heart rate) during the first 10 min of reperfusion tended to be lower in the transgenic hearts (64±2% vs 90±18%, for TG, n=3, and WT, n=6, hearts, respectively; Figure 5D). After 20 min of reperfusion this difference disappeared, the work output being 82±7% (n=3) in the αMyHC-VEGF-B_{167} hearts and 85±18 (n=3) in the controls (Figure 5D).

Both transgenic and wildtype mice responded to angiotensin II (AngII)-induced pressure overload by decreasing left ventricular internal diameter and stroke volume (WT untreated 34.26±4.47µl, WT AngII-treated 28.01±4.48µl, n=6, p<0.05; TG untreated 39.13±5.17µl, TG AngII-treated 28.12±4.47µl, n=6, p<0.01). Furthermore, the AngII-treated transgenic mice did not show any functional impairment when compared to AngII-treated wildtype littermates in echocardiographic analysis, further confirming that the VEGF-B induced hypertrophy does not compromise heart function.

Mitochondrial changes in the transgenic hearts are associated with abnormal lipid accumulation

Despite normal cytochrome concentrations in the transgenic hearts, electron microscopic analysis revealed progressive changes in the structure of cardiomyocyte mitochondria in two and six-month-old transgenic mice (Figure 6A–D, Supplemental Figure 3), including swelling and altered morphology of the cristae (white arrows, Figure 6C), apparently leading to mitochondrial lysis (black arrows). These changes accumulated in older transgenic mice, and intracellular vacuoles were visible in the transgenic hearts in light microscopy at one year of age (arrows in Figure 6E). Mitochondrial changes suggested altered energy metabolism in the cardiomyocytes, which use mainly fatty acids as an energy source.

Previous studies have indicated that increased myocardial fatty acid uptake or decreased fatty acid utilization leads to cardiac hypertrophy followed by the accumulation of toxic lipid species[17, 18]. We therefore carried out lipidomic profiling of the hearts. This analysis revealed a significant increase in *de novo* synthesized ceramide levels in the transgenic hearts, as measured by the ceramide to sphingomyelin ratio (Figure 7A and Supplemental Figure 4), whereas the triacylglycerols were decreased, as normalized to total phospholipid concentrations (Figure 7B) or to tissue weight (data not shown). Ceramides are known for their toxicity and accumulate in pathological conditions such as diabetes mellitus or adipose tissue inflammation[19, 20]. Thus, ceramide accumulation was the probable reason for the morphological changes and increased mortality of the αMyHC-VEGF-B_{167} transgenic mice.

Discussion

In the present study we show that elevated expression of VEGF-B induces very little angiogenesis in the skin or heart, but instead hypertrophy of the cardiac muscle without significant changes in pumping function. As the transgenic blood pressure and heart rate were decreased, the hypertrophy was not a consequence of increased workload, but rather caused by an intrinsic metabolic effect induced by cardiomyocyte expression of VEGF-B. Although the transgenic mice had larger myocardial capillaries, their tolerance to cardiac ischemia and reperfusion as well as to angiotensin II-induced myocardial stress was not compromised. However, evidence was obtained of altered cardiac lipid metabolism, ceramide accumulation, gradual mitochondrial damage, and increased death of the transgenic mice. The unexpected metabolic and trophic effects of VEGF-B in the myocardium and the absence of major angiogenic effects are striking for a member of the VEGF family.

Several studies, including our present results, indicate that VEGF-B is not a major angiogenesis-inducing factor. Instead, VEGF-B may have the ability to potentiate neovascularization in pathological conditions[9]. In this regard VEGF-B differs greatly from PlGF, which also binds to VEGFR-1 and NRP-1 and induces angiogenesis in various tissues, including the heart[21,22]. In the skin, VEGF-B overexpression only slightly increased dermal capillary density. In the VEGF-B overexpressing hearts, vessel density was decreased because of vessel displacement by hypertrophic cardiomyocytes, while vessel diameter was greater so that the total capillary area per cardiomyocyte was increased. VEGF-B staining decorated cardiomyocytes and the pericellular basement membranes, indicating that the transgene was abundantly expressed, and consistent with the finding that VEGF-B_{167} binds to pericellular heparan sulphate[14]. The lack of a significant angiogenic effect is consistent with earlier reports where VEGF-B was expressed in endothelial cells and shown to promote minimal angiogenesis[13].

We detected a progressively increasing heart to body weight ratio in the transgenic mice, which was associated with increased thickness of the cardiac muscle wall. The reason for the increased cardiac mass appeared to be hypertrophy of the cardiomyocytes as determined by increased

cell size, and the transgenic hearts lacked areas of fibrosis or edema. In contrast to forms of human hypertrophic cardiomyopathy, parallel sarcomere orientation was preserved in the transgenic hearts. Increased beta-adrenergic stimulation and systemic hypertension with associated work overload are known to induce a hypertrophic response in the left ventricle, and angiogenesis is known to be essential for overload-induced adaptive cardiac hypertrophy, whereas inhibition of angiogenesis leads to heart failure[23, 24]. The VEGF-B induced hypertrophy was however not related to these conditions as the heart rate and blood pressure were lower in the transgenic mice, and hypertrophy comprised all parts of the myocardium. Otherwise, the anatomy of the heart and the great vessels was normal. The myocardial hypertrophy in the VEGF-B overexpressing hearts contrasts with the loss-of-function phenotype of the VEGF-B knockout mice which have smaller hearts[8], and is consistent with the recent report that adenoviral VEGF-B treatment promotes cardiomyocyte hypertrophy after myocardial infarction[25].

We observed that intracellular vacuoles accumulate in the cardiomyocytes of the transgenic mice. With electron microscopy these were found to be structures left behind from damaged mitochondria, suggesting that mitochondrial energy metabolism is disturbed in the VEGF-B overexpressing hearts. As cardiomyocytes mainly use lipids as an energy source, it was logical to analyze their lipidomic profiles. Indeed, lipidomic analysis revealed significant changes in the lipid composition of the hearts and suggested a likely reason for the cardiac hypertrophy. Previous studies have indicated that excess transport of fatty acids can induce cardiac hypertrophy, which converts to lipotoxicity when the mitochondria cannot use all of the available lipids[17]. In particular, ceramide accumulation is known to induce mitochondrial damage[26] and to play a critical role in the pathogenesis of lipotoxic cardiomyopathy[27]. The increased lipolysis of triacylglycerols is the likely reason for their observed depletion in transgenic hearts, and would also explain the elevated ceramide levels. Higher availability of fatty acids due to lipolysis would lead to increased demand for mitochondrial β-oxidation, while the excess pool of saturated long-chain fatty acids would provide substrate for *de novo* ceramide synthesis[28].

Cardiac hypertrophy has also been described following overexpression of long-chain acyl-CoA synthetase in the heart[29]. In this case, toxic lipid species accumulated in the hearts. Altered lipid metabolism seems to be the likely cause for the cardiac hypertrophy in the VEGF-B transgenic hearts, and via increased ceramide accumulation this would gradually lead to cardiomyocyte damage.

Ceramides are also involved in triggering macroautophagy[30]. The intracellular vacuoles in the transgenic hearts suggest ongoing autophagy, which is a normal process in the heart for removal of damaged cytosolic components[31]. This process is linked both to cardioprotection and lipolysis. A major portion of myocardial intracellular triacylglycerol hydrolysis is lysosomal[32], and lysosomes are involved in autophagosome formation[31]. Moreover, increasing the autophagic capacity of cardiomyocytes decreased apoptosis induction upon ischemia-reperfusion[33]. These two processes, autophagy and lipolysis, both related to lysosomal activities, may link the present observations of protection against ischemic damage, a decrease in myocardial triacylglycerols, and an increase in ceramide. There appears to be a fine balance between the pro-apoptotic and protective actions of ceramide, as ceramide has been shown to attenuate hypoxic cell death[34]. Elevated levels of ceramide could thus at least partly account for the improved cell survival after ischemia in αMyHC-VEGF-B_{167} hearts.

Hearts isolated from αMyHC-VEGF-B_{167} mice showed some protection against cellular damage after ischemia-reperfusion, as evidenced by less LDH release. Nevertheless, there was no significant difference between the αMyHC-VEGF-B_{167} mice and controls in the mechanical work output 25 min after the beginning of reperfusion, although during the first 10 min there

seemed to be a lag in attaining the basal work output. The causal connection between the subdued commencement of contractions upon reperfusion and the decrease in LDH release is unclear. However, in isolated hearts, lower pressure during commencement of reperfusion has been found to protect against injury[35].

We monitored the redox state of mitochondria during variable workload and substrate availability, but no systematic effects of the VEGF-B_{167} overexpression were found (unpublished observations of E.L. and I.H.). The response of the redox state of myocardial cytochrome aa_3 to workload transitions was normal, and the redox level at extrapolated zero workload was similar in the αMyHC-VEGF-B_{167} and control hearts, indicating no difference in mitochondrial energy coupling or basal metabolic rate. Interestingly however, VEGF-B expression was recently found to correlate with that of several mitochondrial genes in a large bioinformatic and proteomic analysis of mitochondrial proteins[36], suggesting that its expression is associated with energy metabolism. A recent study has also indicated that the metabolic sensor peroxisome proliferator-activated receptor-γ coactivator 1α (PGC-1α) regulates VEGF expression and angiogenesis in ischemic tissues[37]. These results shed new light on an important interplay between nutrient demand, metabolism, and vascular supply.

The changes observed in the VEGF-B_{167} overexpressing cardiomyocytes may be triggered by receptor activation in endothelial cells, followed by an as yet undetermined signalling to the cardiomyocytes. The finding that VEGF-B alters cardiomyocyte mitochondria and lipid metabolites in the heart in the absence of overt vessel growth is a new finding for an angiogenic factor. Although in our case the excess of VEGF-B ultimately leads to tissue damage, the potential of VEGF-B to regulate cardiomyocyte energy metabolism during shorter treatment periods may turn out to be useful in attempts to salvage myocardial insufficiency where the myocardial energy sources are defective.

Supplementary Material

Refer to Web version on PubMed Central for supplementary material.

Acknowledgements

We thank Raimo Tuuminen and Karl Lemström for help with quantitative histopathology, Ismo Virtanen and Fang Zhao with electron microscopy, Jenni Huusko with echocardiography, Berndt Enholm with generation of αMyHC-VEGF-B_{167} mice, Jarkko Soronen and Seppo Kaijalainen with RT-PCR, and Sandra Castillo for technical assistance. We also thank the Molecular Imaging Unit for microscope support.

Sources of funding

This study was supported by grants from NIH (5-R01-HL075183-02), Academy of Finland Council of Health (202852, 204312 and 210599) and Novo Nordisk Foundation.

References

1. Shibuya M, Claesson-Welsh L. Signal transduction by VEGF receptors in regulation of angiogenesis and lymphangiogenesis. Exp Cell Res 2006;312(5):549–560. [PubMed: 16336962]
2. Karpanen T, Alitalo K. Molecular biology and pathology of lymphangiogenesis. Annu Rev Pathol 2008;3:367–397. [PubMed: 18039141]
3. Olofsson B, Pajusola K, von Euler G, Chilov D, Alitalo K, Eriksson U. Genomic organization of the mouse and human genes for vascular endothelial growth factor B (VEGF-B) and characterization of a second splice isoform. J. Biol. Chem 1996;271:19310–19317. [PubMed: 8702615]
4. Olofsson B, Korpelainen E, Pepper MS, Mandriota SJ, Aase K, Kumar V, Gunji Y, Jeltsch MM, Shibuya M, Alitalo K, Eriksson U. Vascular endothelial growth factor B (VEGF-B) binds to VEGF

receptor-1 and regulates plasminogen activator activity in endothelial cells. Proc. Natl. Acad. Sci. USA 1998;95:11709–11714. [PubMed: 9751730]

5. Makinen T, Olofsson B, Karpanen T, Hellman U, Soker S, Klagsbrun M, Eriksson U, Alitalo K. Differential binding of vascular endothelial growth factor B splice and proteolytic isoforms to neuropilin-1. J Biol Chem 1999;274(30):21217–21222. [PubMed: 10409677]
6. Aase K, Lymboussaki A, Kaipainen A, Olofsson B, Alitalo K, Eriksson U. Localization of VEGF-B in the mouse embryo suggests a paracrine role of the growth factor in the developing vasculature. Dev Dyn 1999;215(1):12–25. [PubMed: 10340753]
7. Aase K, von Euler G, Li X, Ponten A, Thoren P, Cao R, Cao Y, Olofsson B, Gebre-Medhin S, Pekny M, Alitalo K, Betsholtz C, Eriksson U. Vascular endothelial growth factor-B-deficient mice display an atrial conduction defect. Circulation 2001;104(3):358–364. [PubMed: 11457758]
8. Bellomo D, Headrick JP, Silins GU, Paterson CA, Thomas PS, Gartside M, Mould A, Cahill MM, Tonks ID, Grimmond SM, Townson S, Wells C, Little M, Cummings MC, Hayward NK, Kay GF. Mice lacking the vascular endothelial growth factor-B gene (Vegfb) have smaller hearts, dysfunctional coronary vasculature, and impaired recovery from cardiac ischemia. Circ Res 2000;86(2):E29–E35. [PubMed: 10666423]
9. Mould AW, Tonks ID, Cahill MM, Pettit AR, Thomas R, Hayward NK, Kay GF. Vegfb gene knockout mice display reduced pathology and synovial angiogenesis in both antigen-induced and collagen-induced models of arthritis. Arthritis Rheum 2003;48(9):2660–2669. [PubMed: 13130487]
10. Sun Y, Jin K, Childs JT, Xie L, Mao XO, Greenberg DA. Increased severity of cerebral ischemic injury in vascular endothelial growth factor-B-deficient mice. J Cereb Blood Flow Metab 2004;24 (10):1146–1152. [PubMed: 15529014]
11. Rissanen TT, Markkanen JE, Gruchala M, Heikura T, Puranen A, Kettunen MI, Kholova I, Kauppinen RA, Achen MG, Stacker SA, Alitalo K, Yla-Herttuala S. VEGF-D is the strongest angiogenic and lymphangiogenic effector among VEGFs delivered into skeletal muscle via adenoviruses. Circ Res 2003;92(10):1098–1106. [PubMed: 12714562]
12. Bhardwaj S, Roy H, Gruchala M, Viita H, Kholova I, Kokina I, Achen MG, Stacker SA, Hedman M, Alitalo K, Yla-Herttuala S. Angiogenic responses of vascular endothelial growth factors in periadventitial tissue. Hum Gene Ther 2003;14(15):1451–1462. [PubMed: 14577925]
13. Mould AW, Greco SA, Cahill MM, Tonks ID, Bellomo D, Patterson C, Zournazi A, Nash A, Scotney P, Hayward NK, Kay GF. Transgenic overexpression of vascular endothelial growth factor-B isoforms by endothelial cells potentiates postnatal vessel growth in vivo and in vitro. Circ Res 2005;97 (6):e60–e70. [PubMed: 16109918]
14. Olofsson B, Pajusola K, Kaipainen A, von Euler G, Joukov V, Saksela O, Orpana A, Pettersson RF, Alitalo K, Eriksson U. Vascular endothelial growth factor B, a novel growth factor for endothelial cells. Proc. Natl Acad. Sci. USA 1996;93:2576–2581. [PubMed: 8637916]
15. Butz GM, Davisson RL. Long-term telemetric measurement of cardiovascular parameters in awake mice: a physiological genomics tool. Physiol Genomics 2001;5(2):89–97. [PubMed: 11242593]
16. Kunz WS, Kunz W. Contribution of different enzymes to flavoprotein fluorescence of isolated rat liver mitochondria. Biochim Biophys Acta 1985;841(3):237–246. [PubMed: 4027266]
17. Chiu HC, Kovacs A, Blanton RM, Han X, Courtois M, Weinheimer CJ, Yamada KA, Brunet S, Xu H, Nerbonne JM, Welch MJ, Fettig NM, Sharp TL, Sambandam N, Olson KM, Ory DS, Schaffer JE. Transgenic expression of fatty acid transport protein 1 in the heart causes lipotoxic cardiomyopathy. Circ Res 2005;96(2):225–233. [PubMed: 15618539]
18. Sharma S, Adrogue JV, Golfman L, Uray I, Lemm J, Youker K, Noon GP, Frazier OH, Taegtmeyer H. Intramyocardial lipid accumulation in the failing human heart resembles the lipotoxic rat heart. Faseb J 2004;18(14):1692–1700. [PubMed: 15522914]
19. Kolak M, Westerbacka J, Velagapudi VR, Wagsater D, Yetukuri L, Makkonen J, Rissanen A, Hakkinen AM, Lindell M, Bergholm R, Hamsten A, Eriksson P, Fisher RM, Oresic M, Yki-Jarvinen H. Adipose tissue inflammation and increased ceramide content characterize subjects with high liver fat content independent of obesity. Diabetes 2007;56(8):1960–1968. [PubMed: 17620421]
20. Medina-Gomez G, Gray SL, Yetukuri L, Shimomura K, Virtue S, Campbell M, Curtis RK, Jimenez-Linan M, Blount M, Yeo GS, Lopez M, Seppanen-Laakso T, Ashcroft FM, Oresic M, Vidal-Puig A.

PPAR gamma 2 prevents lipotoxicity by controlling adipose tissue expandability and peripheral lipid metabolism. PLoS Genet 2007;3(4):e64. [PubMed: 17465682]

21. Luttun A, Tjwa M, Moons L, Wu Y, Angelillo-Scherrer A, Liao F, Nagy JA, Hooper A, Priller J, De Klerck B, Compernolle V, Daci E, Bohlen P, Dewerchin M, Herbert JM, Fava R, Matthys P, Carmeliet G, Collen D, Dvorak HF, Hicklin DJ, Carmeliet P. Revascularization of ischemic tissues by PlGF treatment, and inhibition of tumor angiogenesis, arthritis and atherosclerosis by anti-Flt1. Nat Med 2002;8(8):831–840. [PubMed: 12091877]
22. Odorisio T, Schietroma C, Zaccaria ML, Cianfarani F, Tiveron C, Tatangelo L, Failla CM, Zambruno G. Mice overexpressing placenta growth factor exhibit increased vascularization and vessel permeability. J Cell Sci 2002;115(Pt 12):2559–2567. [PubMed: 12045226]
23. Sano M, Minamino T, Toko H, Miyauchi H, Orimo M, Qin Y, Akazawa H, Tateno K, Kayama Y, Harada M, Shimizu I, Asahara T, Hamada H, Tomita S, Molkentin JD, Zou Y, Komuro I. p53-induced inhibition of Hif-1 causes cardiac dysfunction during pressure overload. Nature 2007;446(7134): 444–448. [PubMed: 17334357]
24. Shiojima I, Sato K, Izumiya Y, Schiekofer S, Ito M, Liao R, Colucci WS, Walsh K. Disruption of coordinated cardiac hypertrophy and angiogenesis contributes to the transition to heart failure. J Clin Invest 2005;115(8):2108–2118. [PubMed: 16075055]
25. Tirziu D, Chorianopoulos E, Moodie KL, Palac RT, Zhuang ZW, Tjwa M, Roncal C, Eriksson U, Fu Q, Elfenbein A, Hall AE, Carmeliet P, Moons L, Simons M. Myocardial hypertrophy in the absence of external stimuli is induced by angiogenesis in mice. J Clin Invest 2007;117(11):3188–3197. [PubMed: 17975666]
26. Scarlatti F, Bauvy C, Ventruti A, Sala G, Cluzeaud F, Vandewalle A, Ghidoni R, Codogno P. Ceramide-mediated macroautophagy involves inhibition of protein kinase B and up-regulation of beclin 1. J Biol Chem 2004;279(18):18384–18391. [PubMed: 14970205]
27. Park TS, Hu Y, Noh HL, Drosatos K, Okajima K, Buchanan J, Tuinei J, Homma S, Jiang XC, Abel ED, Goldberg IJ. Ceramide is a cardiotoxin in lipotoxic cardiomyopathy. J Lipid Res. 2008
28. Sparagna GC, Hickson-Bick DL, Buja LM, McMillin JB. A metabolic role for mitochondria in palmitate-induced cardiac myocyte apoptosis. Am J Physiol Heart Circ Physiol 2000;279(5):H2124–H2132. [PubMed: 11045945]
29. Chiu HC, Kovacs A, Ford DA, Hsu FF, Garcia R, Herrero P, Saffitz JE, Schaffer JE. A novel mouse model of lipotoxic cardiomyopathy. J Clin Invest 2001;107(7):813–822. [PubMed: 11285300]
30. Zheng W, Kollmeyer J, Symolon H, Momin A, Munter E, Wang E, Kelly S, Allegood JC, Liu Y, Peng Q, Ramaraju H, Sullards MC, Cabot M, Merrill AH Jr. Ceramides and other bioactive sphingolipid backbones in health and disease: lipidomic analysis, metabolism and roles in membrane structure, dynamics, signaling and autophagy. Biochim Biophys Acta 2006;1758(12):1864–1884. [PubMed: 17052686]
31. Gustafsson AB, Gottlieb RA. Recycle or die: the role of autophagy in cardioprotection. J Mol Cell Cardiol 2008;44(4):654–661. [PubMed: 18353358]
32. Schoonderwoerd K, Broekhoven-Schokker S, Hulsmann WC, Stam H. Involvement of lysosome-like particles in the metabolism of endogenous myocardial triglycerides during ischemia/reperfusion. Uptake and degradation of triglycerides by lysosomes isolated from rat heart. Basic Res Cardiol 1990;85(2):153–163. [PubMed: 2350329]
33. Hamacher-Brady A, Brady NR, Gottlieb RA. Enhancing macroautophagy protects against ischemia/ reperfusion injury in cardiac myocytes. J Biol Chem 2006;281(40):29776–29787. [PubMed: 16882669]
34. Lecour S, Van der Merwe E, Opie LH, Sack MN. Ceramide attenuates hypoxic cell death via reactive oxygen species signaling. J Cardiovasc Pharmacol 2006;47(1):158–163. [PubMed: 16424801]
35. Bopassa JC, Vandroux D, Ovize M, Ferrera R. Controlled reperfusion after hypothermic heart preservation inhibits mitochondrial permeability transition-pore opening and enhances functional recovery. Am J Physiol Heart Circ Physiol 2006;291(5):H2265–H2271. [PubMed: 16798830]
36. Mootha VK, Bunkenborg J, Olsen JV, Hjerrild M, Wisniewski JR, Stahl E, Bolouri MS, Ray HN, Sihag S, Kamal M, Patterson N, Lander ES, Mann M. Integrated analysis of protein composition, tissue diversity, and gene regulation in mouse mitochondria. Cell 2003;115(5):629–640. [PubMed: 14651853]

37. Arany Z, Foo SY, Ma Y, Ruas JL, Bommi-Reddy A, Girnun G, Cooper M, Laznik D, Chinsomboon J, Rangwala SM, Baek KH, Rosenzweig A, Spiegelman BM. HIF-independent regulation of VEGF and angiogenesis by the transcriptional coactivator PGC-1alpha. Nature 2008;451(7181):1008–1012. [PubMed: 18288196]

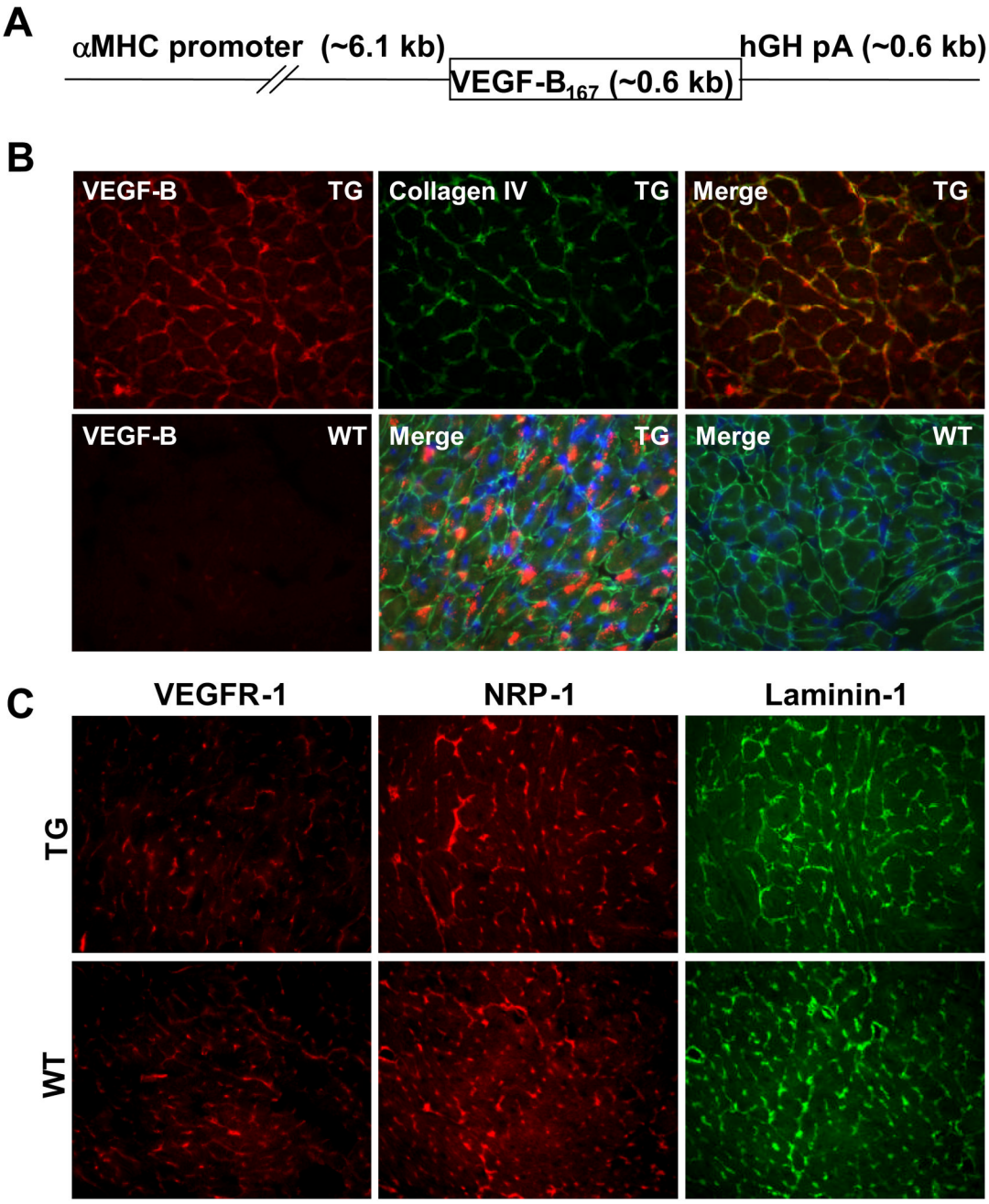

Figure 1. Expression of the αMyHC-VEGF-B$_{167}$ transgene-encoded protein

(**A**) Schematic structure of the αMyHC-VEGF-B$_{167}$ transgene. hGH pA, human growth hormone polyadenylation signal. (**B**) Immunohistochemical staining of heart sections from the αMyHC-VEGF-B$_{167}$ mice (TG) and wildtype littermates (WT) with antibodies against VEGF-B (red) and collagen IV (green). The lower row panels in the middle and far right represent merged figures of permeabilized samples showing intracellular VEGF-B staining. Blue, DAPI staining of nuclei. (**C**) Immunohistochemical staining of heart sections from the αMyHC-VEGF-B$_{167}$ mice (upper row) and littermates (lower row) with antibodies against VEGFR-1 (red), NRP-1 (red) and laminin-1 (green).

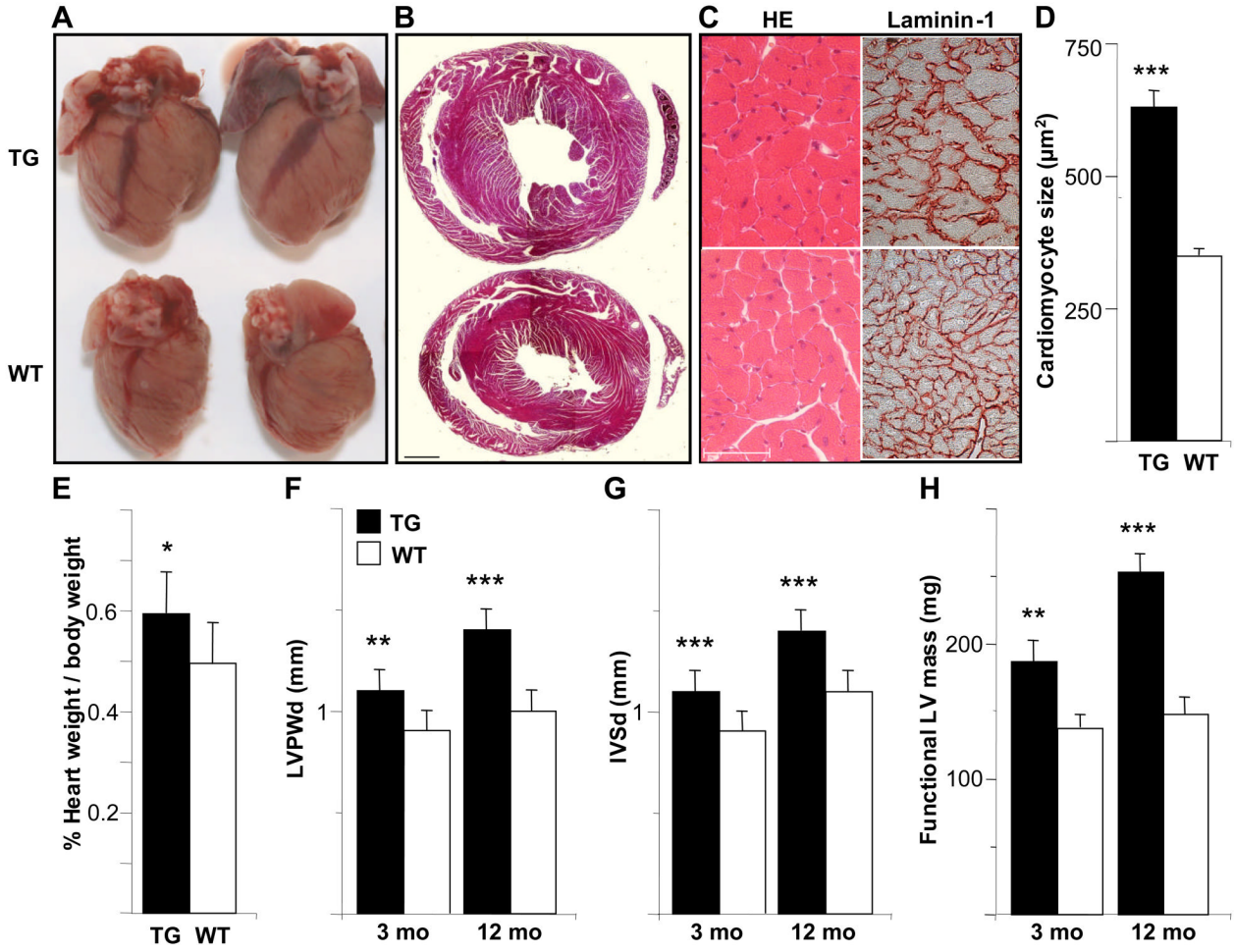

Figure 2. The hearts of the αMyHC-VEGF-B_{167} mice display cardiac hypertrophy, but no significant change in systolic function

(**A**) Ventral view of the hearts from male αMyHC-VEGF-B_{167} mice (upper) and wildtype littermates (lower). (**B**) Hematoxylin-eosin stained heart sections from a male αMyHC-VEGF-B_{167} mouse (upper) and wildtype littermate (lower). Scale bar=1mm. (**C**) Hematoxylin-eosin (HE) and laminin-1 stained heart sections from a male αMyHC-VEGF-B_{167} mouse (upper) and littermate (lower). Scale bar=50μm. (**D**) Size of the myocytes in the αMyHC-VEGF-B_{167} and wildtype hearts (n=10 in both groups). (**E**) Heart weight percentage in male αMyHC-VEGF-B_{167} and wildtype mice. (**F–H**) Thickness of the left ventricular posterior wall (LVPWd, F) and of the interventricular septum (IVSd, G) in diastole and functional left ventricular mass (H) measured by echocardiography in 3- and 12-month(mo)-old male αMyHC-VEGF-B_{167} and wildtype mice. *, p<0.02; **, p<0.01; ***, p<0.001.

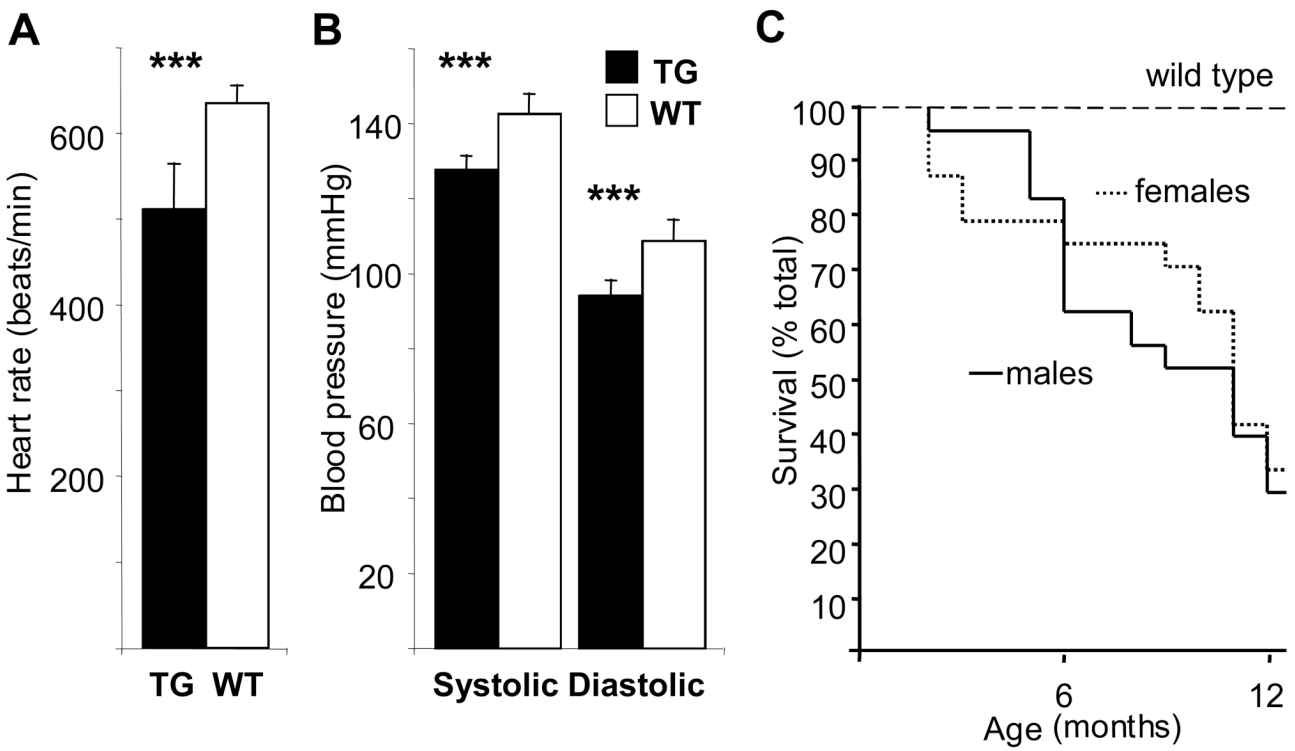

Figure 3. Heart rate, blood pressure and survival of the transgenic and wildtype mice

Telemetric measurements of the heart rate (**A**) as well as systolic and diastolic blood pressure (**B**) of 5-month-old homozygous αMyHC-VEGF-B_{167} male mice and wildtype controls. The values are presented as average±SD. ***, $p<0.001$. (**C**) Transgenic male ($n=24$) and female ($n=27$) mice were followed for 12 months, and incidence of spontaneous death was recorded as a function of time and compared to the previously reported wildtype FVB/N survival (60% at 24 months according to Harlan Sprague Dawley Inc). Data presented as a Kaplan-Meier survival curve.

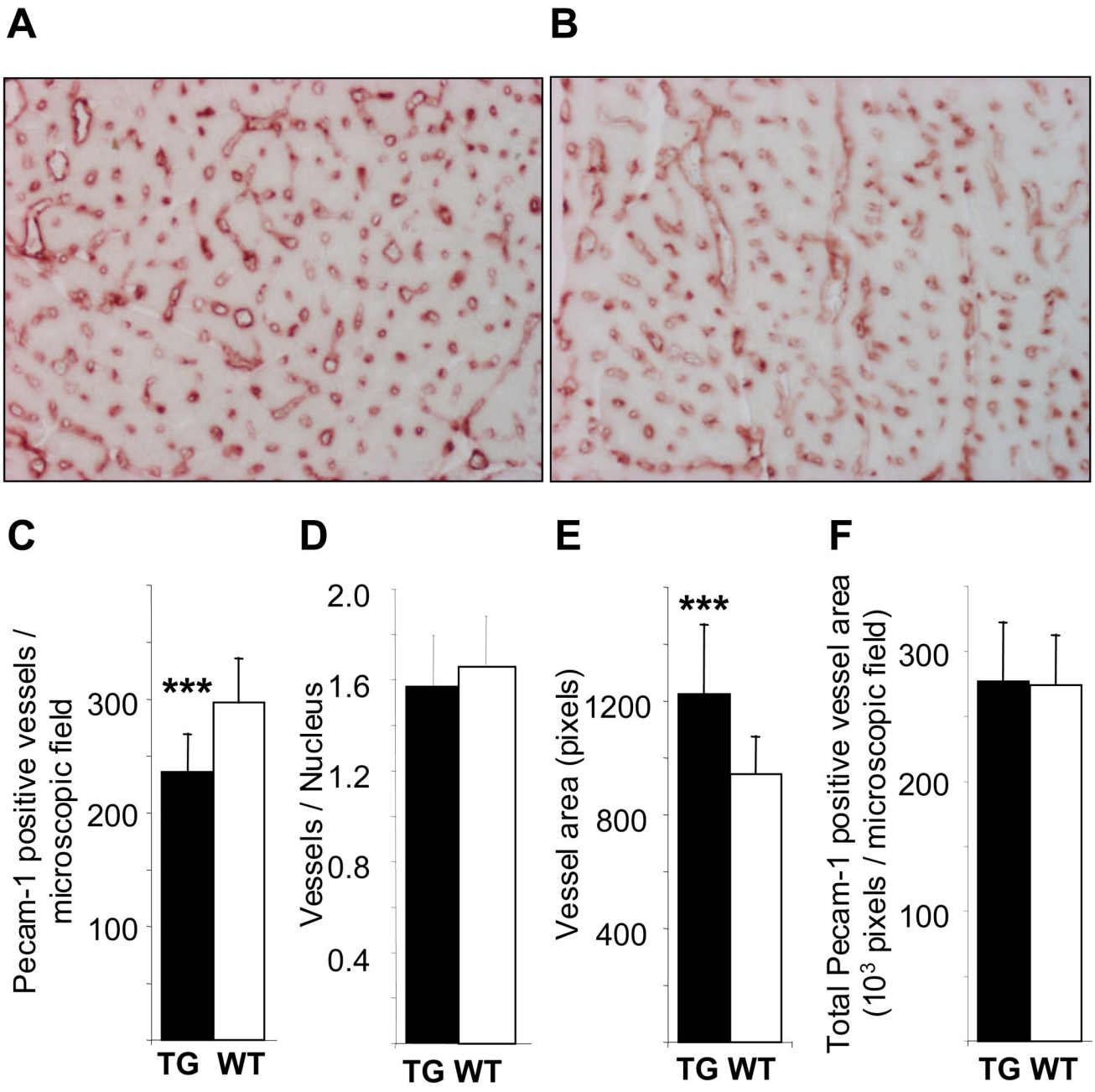

Figure 4. Altered pattern of myocardial capillaries in the αMyHC-VEGF-B$_{167}$ hearts

Sections of the hearts from male αMyHC-VEGF-B$_{167}$ (**A**) and wildtype littermate (**B**) mice were stained with antibodies against Pecam-1, and the number of Pecam-1 positive vessels was quantified (**C**). Number of Pecam-1 positive vessels per cell nucleus (**D**), average area of Pecam-1 positive vessels (**E**), and total area covered by Pecam-1 positive vessels (**F**) in αMyHC-VEGF-B$_{167}$ and wildtype littermates. The values are presented as average±SD. ***, p<0.002.

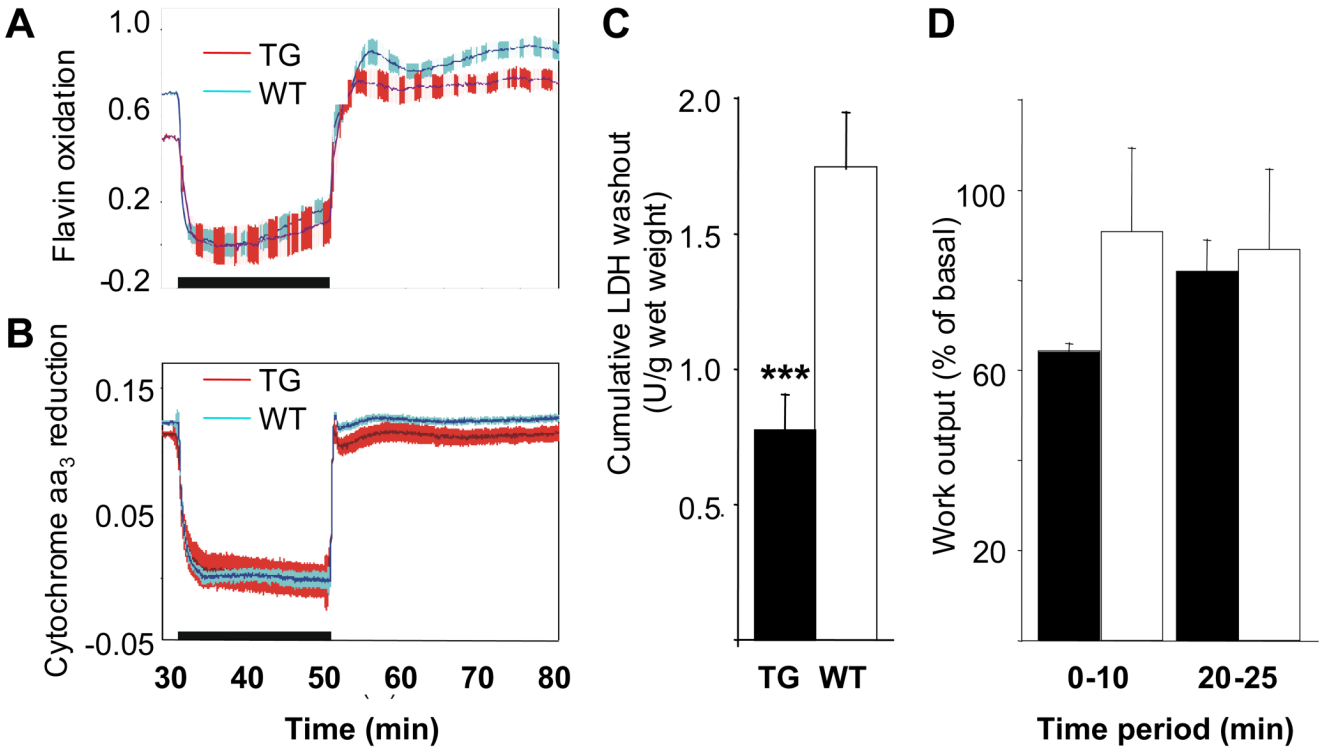

Figure 5. Effects of short-term global ischemia and reperfusion on the hearts of αMyHC-VEGF-B_{167} mice

Oxidation-reduction state of cytochrome *c* oxidase (cytochrome aa_3) (**A**, values on the y-axis present fluorescence increase 465nm-540nm) and fluorescent flavoproteins (**B**, values on the y-axis present fluorescence change 605nm-530nm) in αMyHC-VEGF-B_{167} and control hearts during 20-min global ischemia and reperfusion. The black horizontal bar depicts the time period of ischemia, and in both panels upward deflection indicates oxidation. Red, αMyHC-VEGF-B_{167} (*n*=7), blue, controls (*n*=10). The hatched area represents ±SE. (**C**) Cumulative LDH washout from homozygous αMyHC-VEGF-B_{167} and control mouse hearts during 30 min reperfusion after 20 min of global ischemia. The values are means±SE from 6 and 10 independent experiments, respectively. ***, $p<0.005$. (**D**) Work output from αMyHC-VEGF-B_{167} and wildtype mouse hearts during reperfusion after 20 min of global ischemia. The values are presented as mean±SE from 3 and 6 experiments, respectively.

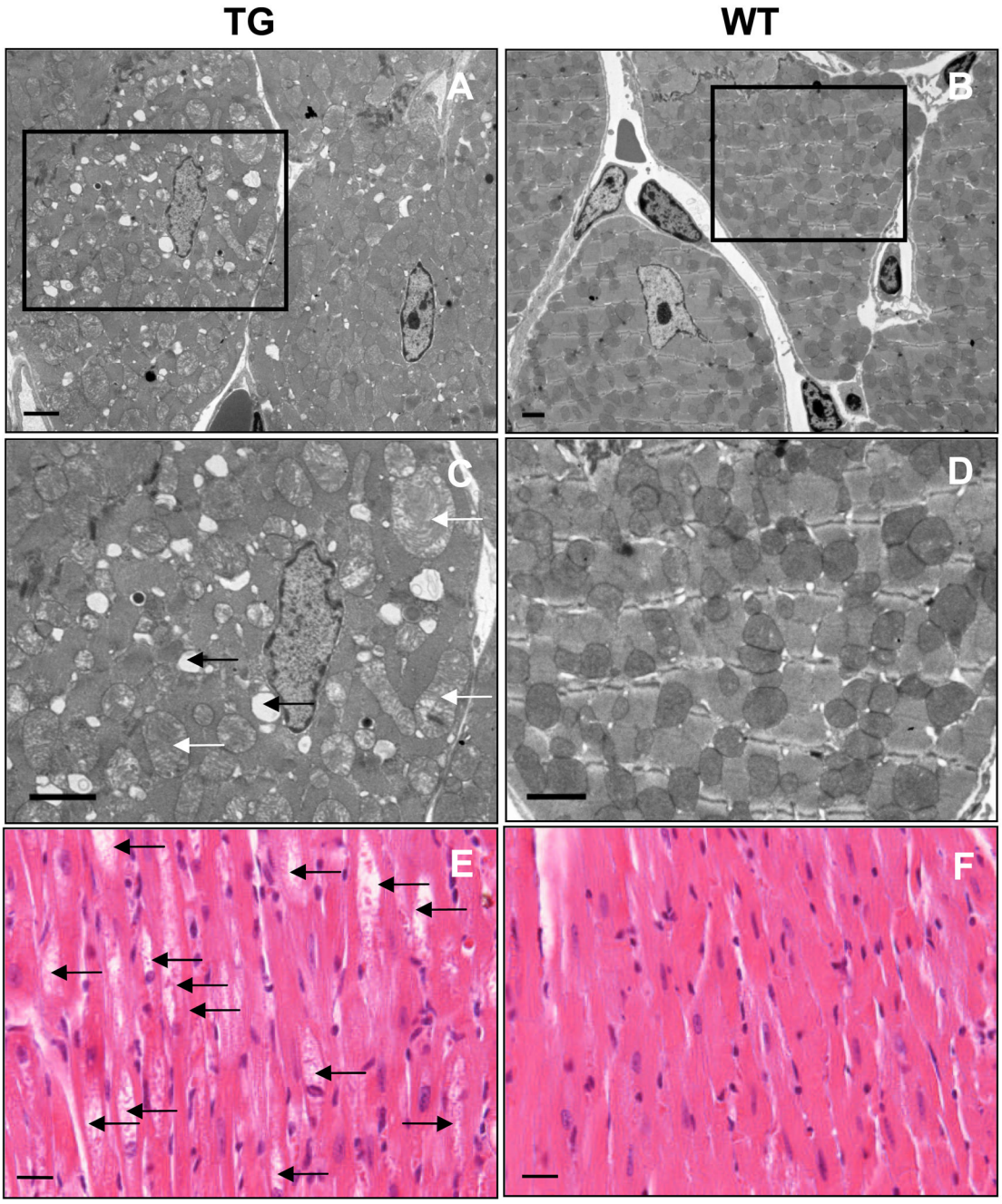

Figure 6. The αMyHC-VEGF-B$_{167}$ mice display abnormal mitochondria and vacuoles in cardiomyocytes

(**A–D**) Transmission electron micrographs displaying mitochondrial morphology in six-month-old αMyHC-VEGF-B$_{167}$ (left) and wildtype (right) control hearts. Scale bar=2μm. (**C–D**) Magnified images of boxed areas in A,B. (**E**) Vacuoles inside cardiomyocytes in 1.5-year-old mice, hematoxylin-eosin staining. Scale bar=50μm.

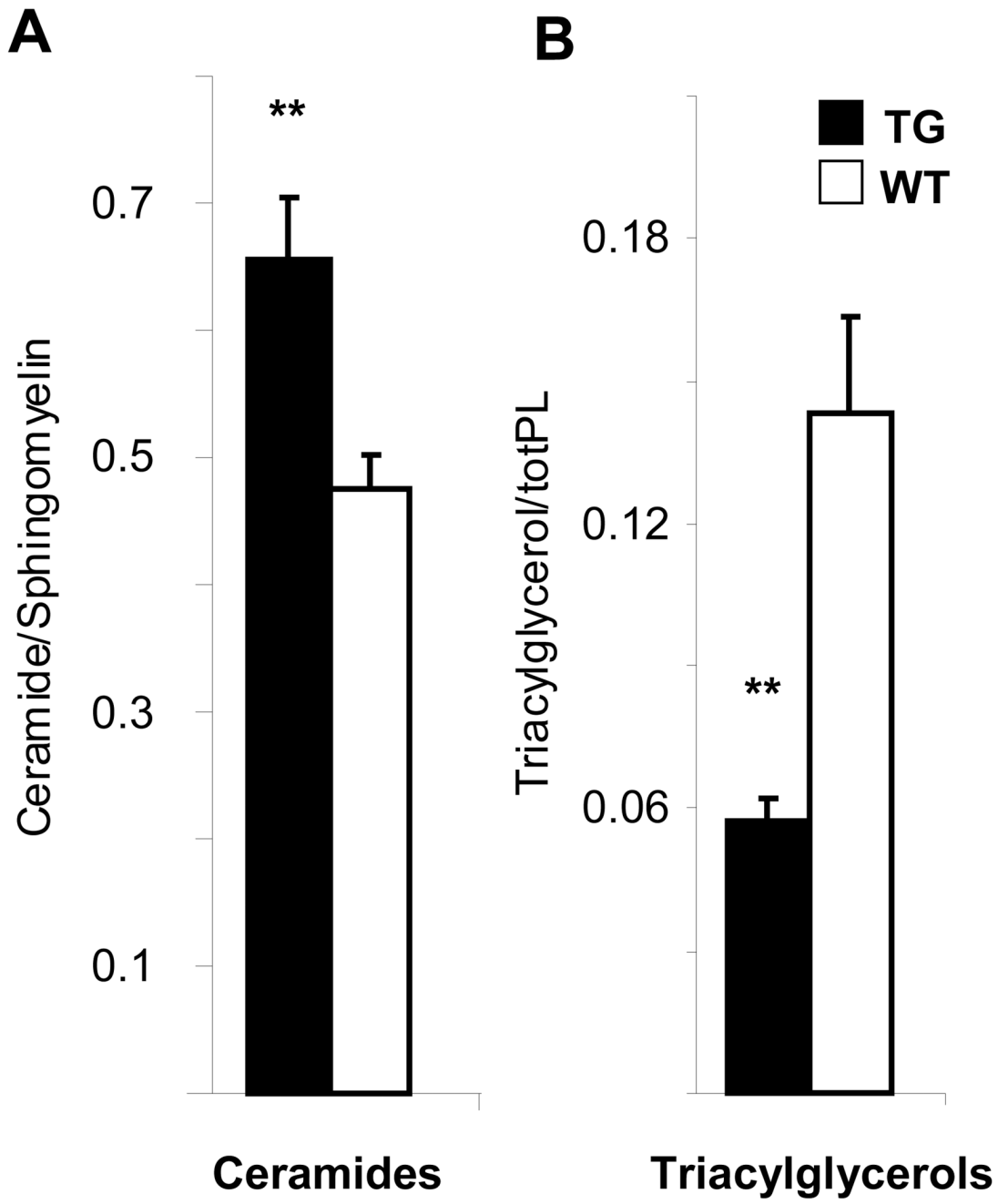

Figure 7. The hearts of the αMyHC-VEGF-B$_{167}$ mice contain an increased amount of ceramides but decreased levels of triacylglycerols

(**A**) The concentration of ceramides to sphingomyelin and (**B**) triacylglycerols to total phospholipid levels in female αMyHC-VEGF-B$_{167}$ (*n*=8) and wildtype (*n*=9) mice. **, $p<0.05$. Values are presented as mean±SEM.

Table 1

Echocardiographic analysis of 3 and 12-month(mo)-old transgenic mice and wildtype littermates.

	3 mo TG	3 mo WT	12 mo TG	12 mo WT
IVSd (mm)	1.1±0.1*	0.9±0.1	1.4±0.1*	1.1±0.1
IVSs (mm)	2.0±0.2*	1.9±0.1	2.2±0.2*	2.0±0.1
LVd (mm)	3.9±0.4	4.0±0.2	3.9±0.3	3.6±0.3
LVs (mm)	1.6±0.3	1.7±0.4	1.8±0.5	1.4±0.6
LVPWd (mm)	1.1±0.1*	0.9±0.1	1.4±0.2*	1.0±0.1
LVPWs (mm)	1.8±0.2*	1.6±0.2	2.0±0.3	1.8±0.2
MWTd (mm)	1.1±0.1*	0.9±0.1	1.4±0.1*	1.1±0.1
MWTs (mm)	1.9±0.2*	1.7±0.1	2.1±0.2*	1.9±0.1
LV FS (%)	60±7	59±8	53±12	63±14
LV EF (%)	93±3	92±4	87±8	93±6
LV mass (mg)	187±41*	137±29	253±40*	148±37
HR (beats/min)	296±40*	416±90	324±28*	377±43

d, diastole; s, systole; IVS, interventricular septum; LV, left ventricle; LVPW, left ventricle posterior wall; MWT, mean wall thickness; FS, fractional shortening; EF, ejection fraction; HR, heart rate. Results are expressed as mean±SD.

* $p<0.05$ vs WT, $n=8–10$ in each group.